PROBING THE CORES OF RADIO JETS THROUGH INTERSTELLAR SCINTILLATION

Barney J. Rickett[1]

RESUMEN

Se ha confirmado que el centelleo interestelar provoca variaciones aleatorias en fuentes compactas de radio en escalas de un día, o menos. Esta interpretación nos proporciona información cuantitativa sobre la estructura de los chorros en radio en las regiones internas de las fuents, en escalas que llegan hasta 10μarcsec si se conoce la distancia a la región que produce la dispersión. A su vez, estos valores implican factores de Doppler de 5-75, que son del mismo orden que aquellos derivaods de interferometría VLB.

ABSTRACT

Interstellar Scintillation (ISS) has been established as the cause of the random variations in compact radio radio sources on times of a day or less. This interpretation provides quantitative information on the structure of the inner regions of the Radio-Emitting Jets on scales down to 10μarcsec, once the distance to the scattering region is known. In turn these imply Doppler factors 5-75, which are on the same order as derived from VLB interferometry.

1. INTRA-DAY VARIABILITY

Intraday variability (IDV) of extra-galactic sources at frequencies below about 10 GHz is due to Interstellar Scintillation (ISS). This statement would have been controversial, even 5 years ago, but is now accepted by the great majority of those familiar with the subject. In this paper I review the evidence and show how ISS allows quantitative conclusions to be drawn about both the radio structure of the brightest radio-emitting features and the interstellar medium responsible for the rapid variations in flux density.

IDV was discovered at cm wavelengths by the Bonn group (Heeschen et al. 1987a). For example Quirrenbach et al. (1989) found that the 6 cm flux density of quasar B0917+624 varied by more than 10% in a day. Since then timescales shorter than one hour have been observed from a few sources (e.g. Kedziora-Chudczer et al. 1997; Dennett-Thorpe & de Bruyn 2000) – which could be called intra-hour variables (IHV). If IDV or IHV were intrinsic the implied brightness temperatures would be $10^{18} - 10^{21}$ K), which require Doppler factors of 50-200 over the inverse Compton limit of 10^{12} K. The intrinsic interpretation triggered considerable interest in the IDV phenomenon and many papers were published proposing extreme physics such as coherent radio emission and various shocked jets.

Possible extrinsic explanations were also considered, namely gravitational lensing or ISS, and the latter is now the accepted explanation since many of the phenomena expected for ISS have been observed in the last ten years.

2. INTERSTELLAR SCINTILLATION AS THE CAUSE OF IDV

The phenomenon of interstellar scattering is a central fact in the observations of pulsars. It broadens the pulses and randomly modulates their amplitudes. This random modulation (called scintillation) is characterized by the typical timescale and bandwidth over which the amplitudes become decorrelated. These scales vary strongly with wavelength, because the refractive index of the interstellar plasma is dispersive, causing more scattering with increasing wavelength and also with increasing path length in the plasma. The scintillation can be weak with modulation index (rms/mean intensity) $m < 1$ or strong with $m > 1$, and in the latter case there are diffractive and refractive modulations which have differring characteristic scales. The IDV phenomenon is typically observed near the transition frequency that separates weak from strong ISS. At that frequency or above the dominant spatial scale in the diffraction pattern is the Fresnel scale $r_F = \sqrt{L\lambda/2\pi}$, where L is the distance from the ob-
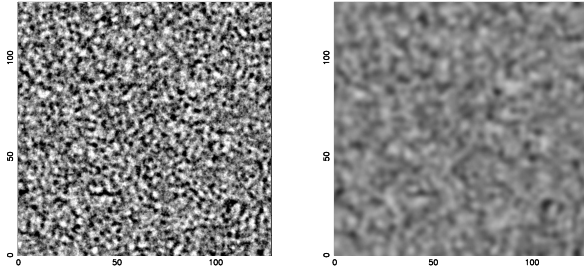
[1]University of California, San Diego, CA, USA.

Fig. 1. Simulation in weak scintillation caused by propagation through a random phase screen at distance L, described by a Kolmogorov wavenumber spectrum of density fluctuations. The intensity is shown by the grayscale (darker meaning stronger) saturating in white at zero intensity and in black at three times rms above the mean of the left panel. Left panel: for a point source. Right panel: for an extended source that subtends three times the angle subtended by the Fresnel scale ($\theta_F = r_F/L$). The axes are marked in units of the Fresnel scale.
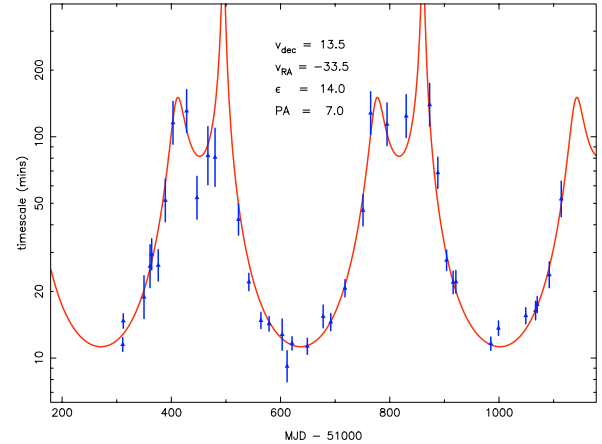

Fig. 2. The characteristic timescale of the IDV at 5 GHz from quasar J1819+385 over 1000 days from Jan 1 1999. The fitted model has an elliptical Gaussian correlation function with an axial ratio of 14:1 and a velocity of 36 km/s for the scattering medium (relative to the local standard of rest) from Dennett-Thorpe & de Bruyn (2003).

server to the scattering layer and λ is the observing wavelength.

From thirty-five years of pulsar observations a picture has emerged of how the Galactic electrons are distributed. They are mostly in a warm ($\sim 10^4$ K) ionized component of the interstellar medium which appears to be turbulent over scales from 100 km to more than 10 AU (e.g. Armstrong, Rickett, & Spangler 1995). Taylor & Cordes (1993) assembled the data into the first systematic model for the electron distribution. Cordes & Lazio (2002) have now updated that in a model they call "NE2001".

The radio waves from an AGN propagate through the Galactic electrons and are scattered and scintillate, like the light from a star is scattered in the Earth's atmosphere and appears to twinkle. Just as planets dont twinkle, most radio sources have angular diameters too large to scintillate. Figure 1 shows a simulation of this effect; as the source size increases the rms variation in amplitude is reduced and the characteristic scale is increased, eventually rendering the amplitude constant. It is of course this same effect that suppresses ISS in normal radio sources, which have larger angular diameters than do pulsars.

However, there are some very compact parts of some AGNs which do scintillate. Below about 1 GHz this causes low frequency variability (Rickett, Coles, & Bourgois 1984; Blandford & Narayan 1985; Rickett 1986). At frequencies of 3-8 GHz it can cause intraday variation in flux density. Heeschen & Rickett (1987b) reported early clues to this in the Galactic latitude dependence of the IDV modulation index.

Strong evidence was given by Rickett et al. (1995) that the IDV of quasar B0917+624 was due to ISS, from the partial correlation in the time series across 2:1 ranges in wavelength and in the way the timescale varied with wavelength. This was important because B0917+624 is in many ways the archetype of IDV. Nevertheless, intrinsic IDV contributions at cm wavelengths were still argued by several authors (e.g. Wagner et al. 1996; Kraus et al. 1999; Qian et al. 2002)

Definitive evidence for ISS came from the detection of a time delay on the order of minutes in the IDV observed across inter-continental baselines, and in the detection of annual changes in the characteristic timescale. Both of these phenomena have been seen in the most rapidly varying (IHV) sources, and neither can be explained by intrinsic variability nor by gravitational lensing.

The most dramatic IHV source is the quasar J1819+385, reported by Dennett-Thorpe & de Bruyn (2000). They observed modulation indices of 30% on timescales as short as one hour at 5 GHz, with the timescale changing dramatically over the year. The characteristic ISS timescale is determined by the characteristic spatial scale of the random ISS intensity pattern divided by the velocity of the pattern relative to the Earth. The annual modulation is mostly due to the change in this velocity as the Earth orbits the Sun. It happens that during win-
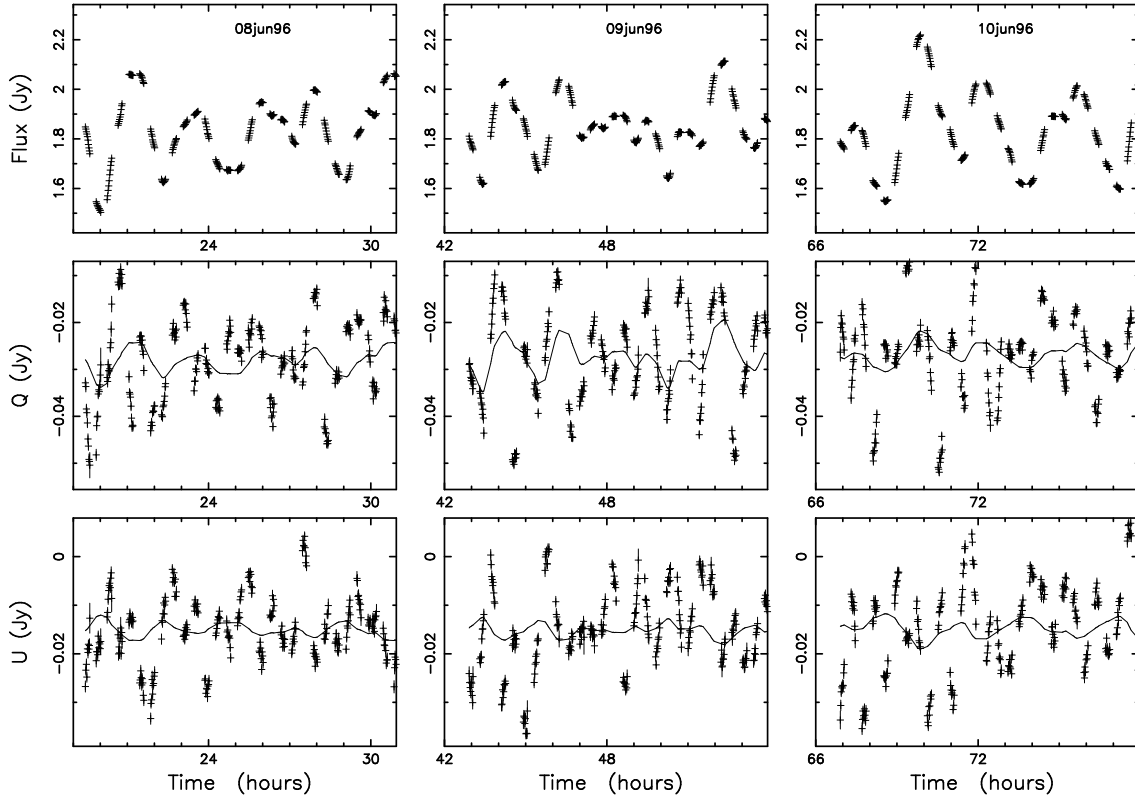
Fig. 3. Time series for I, Q, U from quasar B0405-385 with 1σ errors at 8.6 GHz for June 8-10, 1996. Times are relative to 0hr UT on June 7. The thin solid lines (best fits of the variations in I to the variations in Q and U) represent the expected variability due a polarized point source or a linearly polarized extended source with uniform degree and angle of polarization.

ter and spring the net pattern velocity is fast (short timescale) and in summer and fall the velocity is slow (long timescale). Figure 2 (from Dennett-Thorpe & de Bruyn (2003) shows their observed timescale over a 2.7 year period. They found it necessary to include anisotropy in the spatial model in order to fit the flat-topped shape of the timescale curve. The model shown is highly anisotropic wth an axial ratio of 14:1. Since then several other quasars have shown annual modulations in their timescales, including B0917+624 (Rickett et al. 2001; Jauncey & Macquart 2001) and B1257-326 (Bignall et al. 2003).

The second definitive signature of ISS is the detection of a delay in the ISS across an intercontinental baseline. The best example is again from the IHV quasar J1819+385, reported by Dennett-Thorpe & de Bruyn (2002). At 5 GHz they found the "light curves" observed across 6000 km baseline to be highly correlated and offset by up to 2 minutes. From this they estimated a velocity of the Earth relative to the scintillation pattern of ($\sim$ 50 km/s –

of the same order as cited above. Inter continental time offsets have also been detected for IHV sources B0405-385 and B1257-326 (see Bignall et al. 2003).

3. INTRA-HOUR VARIABLES

The first report of IHV was by Kedziora-Chudczer et al. (1997). They observed hour-long characteristic times for the total flux density at 4.8 and 8.4 GHz for the quasar B0405-385, but they also observed random variations in the linear Stokes' parameters (Q, U) on half-hour timescales, as shown in Figure 3. In the simplest interpretation such rapid changes in polarized flux density could not be due to ISS, because the radio observing frequencies are so far above the interstellar cyclotron frequency, that the medium does not alter the polarization state of a plane wave across the Fresnel scale.

Nevertheless, if the polarization of the source has structure on scales as small as the Fresnel angle ($\theta_F = r_{F/L}$) in the ISM, there can be substantial variations in the observed polarization state on time scale as short as half of the timsecale for in-
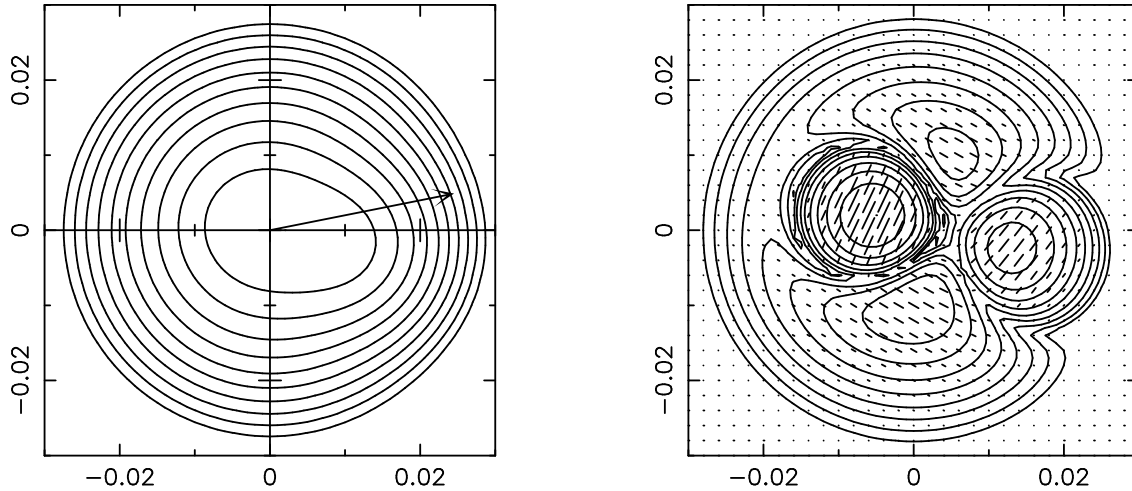
Fig. 4. Model for the brightness distributions for quasar B0405-385 (angles in mas). The left panel shows the total flux density I with the peak brightness about 2×10^{13}K. The right panel shows the polarization with the contours showing total polarized brightness P with maximum $\sim 70\%$ of I; the bars indicate position angle as well as P.

tensity variation. This is due to the fact that the scintillation of waves from source components offset by an angle on the order of the Fresnel angle will only be partially correlated. The summation of such offset patterns with differing polarization causes the net observed polarization state to fluctuate. Indeed Rickett, Kedziora-Chudczer, & Jauncey (2002) were able to find a model for the polarized substructure in the compact core of B0405-385 that gave agreement with the observed correlation functions between Stokes' parameters $I, Q \& U$. The source model shown in Figure 4 is about $20 \times 30 \mu$arcsec with a changing degree of linear polarization angle across the longer dimension. Its maximum apparent brightness is 2×10^{13}K with a 70% degree of polarization. Whereas this model is far from unique, it demonstrates that ISS can explain the statistics of the observed fluctuation in polarization.

It is remarkable that the 30μarcsec estimated angular size of the brightest component in B0405-385 is smaller than can be resolved with current interferometers at cm wavelengths. This emission is presumed to be Doppler-boosted in a jet beamed toward the Earth which increases the brightness temperature $\propto [\delta/(1 + z)]^{1.2}$ (where δ is the Doppler factor and $z = 1.28$ is the quasar redshift; e.g. Marscher 1998) Hence the derived brightness temperature $(2 \times 10^{13}$K) would require a Doppler factor of about 75 if the comoving brightness temperature $\sim 3 \times 10^{11}$K. While this is large it is at the upper end of the Doppler factors estimated from VLBI

imaging of other quasars and AGNs. Thus this polarized IDV does not require a separate explanation over that needed for the images obtained from VLBI.

By considering simultaneously the time scale and modulation index of the ISS Rickett et al. (2002) were able to constrain both the core diameter of the source (θ_c) and the distance (L) to the interstellar scattering. In contrast analysis of the timescale τ_{iss} alone only constrains their product as:

$$\tau_{\text{iss}} \sim 0.002 L_{\text{pc}} \theta_{c, \mu \text{as}} \text{ hrs,} \qquad (1)$$

where a velocity of ~ 30 km/s is assumed for the scattering electrons relative to the Earth. They concluded that the scattering region for B0405-385 was no further than about 30 pc from the Earth and the source diameter was no smaller than about 30μarcsec. If L were larger due to scattering in the 500 pc Galactic disk of electrons, the angular diameter would be proportionately smaller and again require extreme source physics. Since all IHV sources have similarly small values of τ_{iss}, the B0405-385 analysis puts the local origin of the scattering implied for IHV sources on a quantitative footing.

Yet another conclusion for IHV of B0405-385 is illustrated in Figure 5. The auto-correlations of the intensity show a pronounced oscillatory appearance. At these frequencies weak scintillation theory can be used allowing theoretical auto-correlations to be overplotted. The line thickness indicates the axial ratio from thickest to thinnest: 4.0, 2.0, 1.0 and 0.5, where values greater than one correspond to an
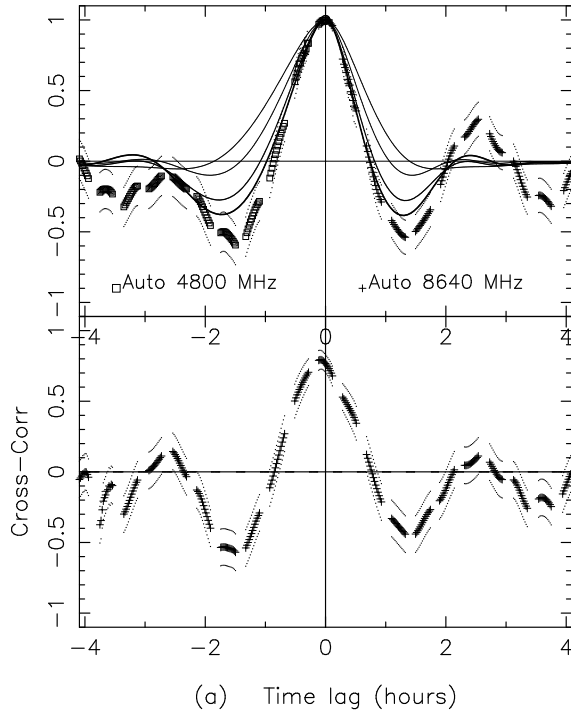
MASIV Survey1 Jan 2002

Fig. 5. Auto- and cross-correlations of total intensity observed for quasar B0405-385 at 8640 and 4800 MHz, plotted against positive and negative time lag, respectively. The $\pm 1\sigma$ errors are plotted as dots above and below. The theoretical acf curves are overplotted for screen models by lines, whose thickness indicates the axial ratio from thickest to thinnest: 0.25, 0.5, 1.0 and 2.0.
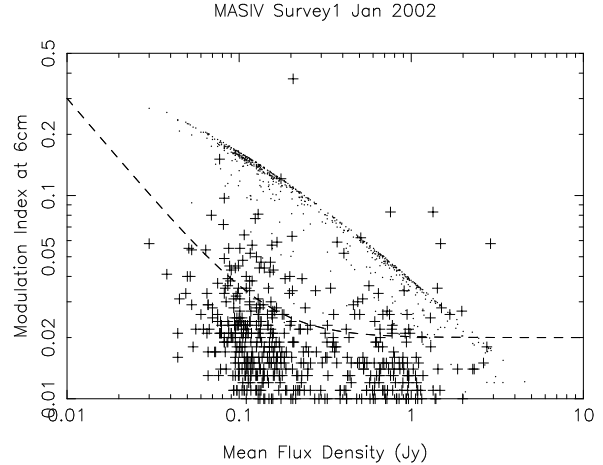
Fig. 6. Modulation index as a function of mean flux density on logarithmic scales. Plus symbols are the MASIV observations at 4.9 GHz. Dots are the predictions for the same sources assuming that each has half of its mean flux in a compact core with a 10^{12}K – see text for details. The variable sources (lying above the dashed threshold line) must have brightnesses higher than 10^{11}K, for which the predicted m values are reduced by a factor $\sqrt{10}$. Though the observations do not follow the tight inverse relation shown by the dots, there is a greater fraction of variable sources weaker than 300 mJy than there is of sources stronger than 300 mJy. The high point at $m = 0.38, \bar{S} = 0.2 Jy$ is the IHV quasar J1819+385, which is thought to show ISS due to enhanced turbulence in a region only 4-20 pc from the Earth. Note the absence of other strongly scintillating sources.

orientation of the effective velocity along the narrow dimension of the anisotropic plasma structures. The conclusion is that the oscillatory appearance can only be matched by this orientation with axial ratios of 4 or more. Once again we obtain a quantitative interpretation of the IHV in terms of scintillation, but there is also a consequence for study of fine structure in the interstellar plasma, since the structure is presumed to be elongated along the local magnetic field.

4. SURVEY FOR MICRO-ARCSECOND SCINTILLATION INDUCED VARIABILITY (MASIV)

While observations prior to 2002 had detected IHV and IDV from about 20 quasars and AGNs at frequencies of 5 GHz and above (e.g. see Quirrenbach et al. 1992), a search for new IDV sources was carried out at the VLA in 2002 by Lovell et al. (2003). 710 flat spectrum sources above a declination of 35 deg were monitored at 2 hour intervals for 72 hours, using the VLA split into five sub-

arrrays. Each source was observed at 4.9 GHz for 1 min, while above an elevation of 15 deg in two subsets – sources stronger than 300 mJy and weaker ones with flux density 130-300 mJy. In Figure 6 the plus symbols show the observed modulation index (m) against mean flux density, with a dashed curve drawn at twice the expected rms due to noise and estimation error. We classified the 99 sources above the line as variable, but 14 showed apparent variation due to baseline rotation and resolved source structure and were discarded. Thus 85 of the 710 sources (12%) were found to vary on timescales from 2 hrs to $\gtrsim 3$ days.

From the distribution of the sources in this figure it appears that there are variables from the sources weaker than 300 mJy than from the stronger sources. Indeed the numbers give 9% of the weaker sources as highly variable ($m > 4\%$) and only 2.5% of the stronger sources as highly variable. Of course this is as expected for sources that tend to be limited to a maximum brightness temperature – weaker sources

then have smaller diameters and so are more likely to show ISS. Figure 6 compares the observed with the predicted distribution under a simulation in which each source has a half of its flux density in a compact "core" with peak brightness of 10^{12}K. The prediction for each source is obtained by a line-of-sight integral of the scintillation variance under the low wavenumber approximation assuming a Kolmogorov spectrum for the electron density (see Coles et al. 1987; Rickett, Lazio, & Ghigo 2005). The weighting along the line of sight is obtained from the Taylor & Cordes (1993) model for the distribution of electrons in the Galaxy. Very similar predictions are obtained from the more recent Cordes & Lazio (2002) model. We conclude that the variable sources have very comapct components (presumably at the base of their jets) with brightness temperatures in the neighbourhood of 10^{12}K and are scintillating in the broad disc of electrons (500 pc scale height) described in th Galactic electron models.

When we undertook the survey we were expecting to find more sources showing dramatic IHV. However, there is only one source with modulation index above about 18%. It is the well known IHV quasar J1819+385, which was by chance included in the survey definition criteria. It shows $m \sim 0.38$ which as we have already discussed must be caused in a scattering region much closer than the 500 pc disc. The absence of many new rapid scintillators seems to be evidence that the fraction of the sky covered by local (tens of pc distant) clouds must be quite small.

5. ISS IN 2 GHZ MONITORING OBSERVATIONS OF AGNS AT GREEN BANK

Because the refractive index in the interstellar plasma depends on frequency (i.e. the medium is dispersive), ISS phenomena also depend on frequency, becoming stronger at lower frequencies. While IDV/IHV are typically observed near 4-8 GHz, there are comparable variations at lower frequencies, which are definitely in the realm of strong ISS, as observed for pulsars. However, the fact that extra-galactic sources have larger angular diameters than pulsars smoothes out the rapid (diffractive ISS) and leaves the slower variations (refractive RISS). Thus at 2 GHz extra-galactic sources scintillate more slowly than at 8 GHz. Intraday variation becomes "intra-week" variation. At still lower frequencies it becomes "low frequency variation" on timescales of months to years (Rickett, Coles, & Bourgois 1984).

From 1979–1996 the Green Bank Interferometer was used by the Naval Research Laboratory to monitor the flux density from 146 compact radio sources
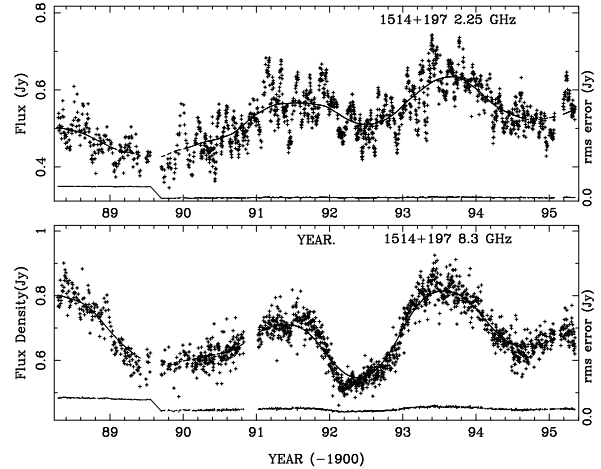

Fig. 7. Green Bank observations of the flux density of BL Lac source B1514+197 at 2.25 and 8.3 GHz sampled every day for 7 years. The solid curve is a running mean estimated over one year, which describes the intrinsic variation. It shows bursts at 8 GHz with larger amplitudes and occurring somewhat earlier than at 2 GHz, as expected for an expanding synchrotron burst. The ISS is the rapid (5-day) variation about the slower intrinsic light curve.

at frequencies near 2 and 8 GHz, as described by Waltman et al. (1991) and Lazio et al. (2001). The "light curves" sampled every one or two days from 1979 to 1996, were re-analyzed by Rickett, Lazio, & Ghigo (2005) to quantify the contribution of ISS to the variations. They were able to separate intrinsic variations on times of a year or more from more rapid ISS on times of 5–50 d by applying low-pass and high-pass filters.

As an example Figure 7 shows the light curves for the BL Lac object B1514+197. The intrinsic variation is represented by the solid lines showing the running mean over one year. These curves show reduced amplitude at 2 GHz and a delay relative to 8 GHz, consistent with models of expanding synchrotron bursts. The ISS are shown by the more rapid deviations about these lines and are much stronger at 2 than at 8 GHz. The ISS is characterized by an rms amplitude and a timescale for every source, from which 121 sources were found to have significant ISS at 2 GHz. Their ISS modulation indices m_2 are in the range 1-10%. m_2 is found to be correlated with the source's flux density exponent α ($S \propto f^\alpha$) and to increase systematically with low Galactic latitude and increased emission measure in that direction (as measured by the Wisconsin Hα maps; Haffner et al. 2003). These relations empha-
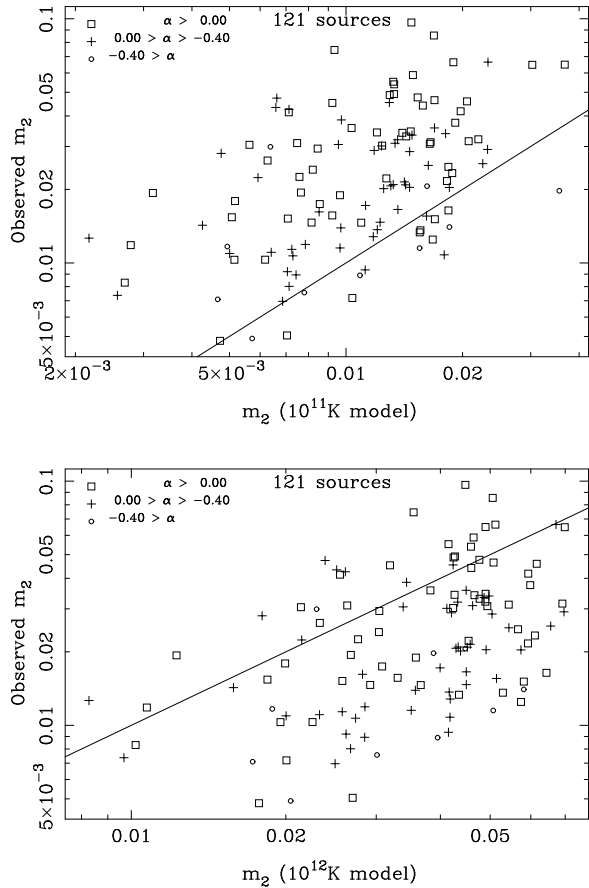
Fig. 8. Observed ISS index m_2 at 2 GHz plotted against the model predictions. In the two models shown half of each source flux density is assumed to be a Gaussian "core" whose peak brightness is 10^{11} K and 10^{12} K on the upper and lower, respectively. The points are flagged by spectral index ($S \propto \nu^\alpha$) as indicated. The solid lines denote observation equal to prediction.

size that the ISS responds to both the peak brightness of the cores of the sources and the column density of electrons in that direction.

Consequently, we modelled the ISS in a fashion similar to that done for the MASIV sources assuming that each has half of its mean flux density in a compact core with a peak brightness of 10^{11}K and 10^{12}K and assuming the Cordes & Lazio (2002) electron distribution. Figure 8 shows the observed m_2 plotted against the predicted values for these two source models. The observed m_2 for the flat spectrum sources are typically above the predictions for the lower brightness model but they are in approximate agreement for the 10^{12}K model. Thus our results are consistent with cm-wavelength VLBI studies of compact AGNs. Though the detailed correla-

tion is poor, presumably due to wide deviations from source to source in the fraction of their flux density in their comapct cores, the conclusion is strong that the maximum brightness temperatures are consistent with the synchrotron self-absorption limit at 3×10^{11} K, boosted in jet configurations by Doppler factors up to about 10.

The average of the observed 2 GHz ISS timescales were in reasonable agreement with the model at Galactic latitudes above about 10 deg. At lower latitudes the observed timescales are too fast, suggesting that the transverse velocity increases beyond about 1 kpc, probably due to differential Galactic rotation, which was not included in the model.

6. A SEARCH FOR SCINTILLATION ARCS FROM QUASAR J1819+385

Stinebring et al. (2001) made an important discovery in the ISS of pulsars, that can also be used as a probe for small scale structure in extra-galactic sources. In pulsar work we study ISS as a function of frequency as well as of time and commonly display it as a dynamic spectrum, as in the left panel of Figure 9 showing the rapidly changing ISS spectrum. The discovery they made was that when such an "image" is subject to two-dimensional Fourier analysis, the resulting power spectrum often shows parabolic features called arcs. This is shown in the right panel and is referred to as the secondary spectrum versus a time coordinate f_ν and a frequency coordinate f_t. It must be plotted with a logarithmic grayscale to reveal the faint arcs. A single point in this plane represents a sinusoidal fringe in the primary dynamic spectrum, which would be caused by the interference of a pair of scattered waves arriving from different angles ($\boldsymbol{\theta_1}, \boldsymbol{\theta_2}$).

These two waves suffer different time delays and different Doppler shifts. The Dopplers differ due to the slightly different rates of change of phase along the two scattered paths due to the transverse motion of the scattering irregularities. The differences in time delay give $f_\nu \propto (\theta_1^2 - \theta_2^2)$ and the differences in Doppler shift are $f_t \propto (\boldsymbol{\theta_1} - \boldsymbol{\theta_2}) \cdot \boldsymbol{V}$, where $\boldsymbol{V}$ is the velocity of the scattering medium relative to the line from the pulsar to the observer. It is these quadratic relations between f_ν and f_t which give rise to the arc phenomenon; in particular if one of the angles is close to zero, as when there is a substantial undeviated component, the relation becomes a parabola (see Cordes et al. 2006 for a discussion of the theory).

Like other scintillation phenomena, arcs will be suppressed if the source is extended (radius $\theta_{\rm src}$).
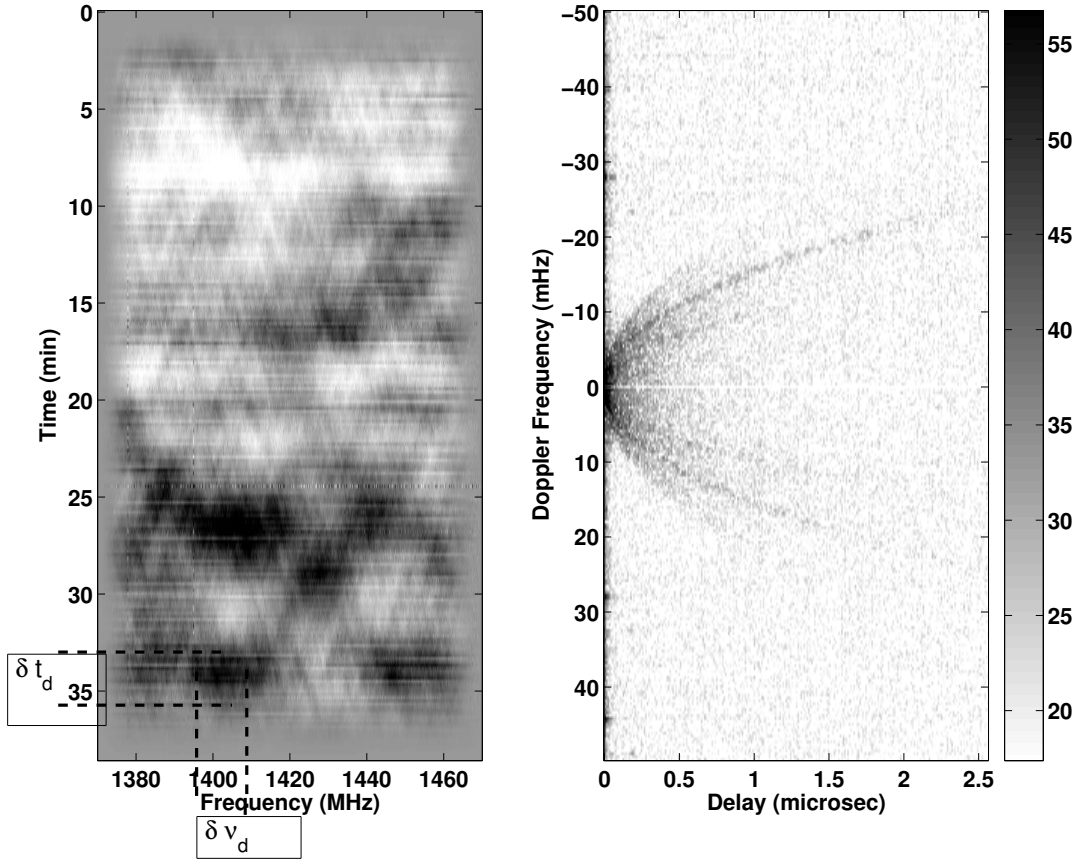
Fig. 9. *Left:* Dynamic spectrum of PSR B1133+16 recorded by Stinebring at Arecibo on modified Julian Date 53224; the darkness of the grayscale is linear in intensity. *Right:* The secondary spectrum (S_2) of the data on the left (its 2-D Fourier power spectrum). The grayscale is logarithmic over 65 dB, revealing remarkable fine parabolic arcs visible out to delays much larger than τ_d, which is the width in delay of the dark region near the origin.

The simplest analysis cuts off the scintillation for $f_t \gtrsim V/(L\theta_{\mathrm{src}})$, due to the smoothing of the diffraction pattern over a scale $L\theta_{\mathrm{src}}$. The fact that pulsar arcs can be seen at f_t values several times larger than the characteristic width for diffractive scintillations means that arcs are a probe for extremely fine source structure.

Macquart & de Bruyn (2005, hereafter MdB) have observed IDV from quasar J1819+385 in relatively wide bandwidths centered on 1.4 GHz. They found that the ISS showed significant variations in the ISS across 160 MHz and even more variation across 600 MHz. They interpret these as diffractive ISS in a scattering layer within 4-15 pc of the Earth and deduce the presence of an ultra compact component in the emission with a minimum brightness temperature of $\sim 10^{14}$K. Thus they argue that this quasar in particular may require a coherent emission mechanism. These authors have graciously given

me access to their 160 MHz bandwidth observations from 2003, from which I have searched for evidence of arcs.

Figure 10 shows the results from 12 april 2003. The dynamic spectrum (left panel) exhibits strong flux density variations of about 150 mJy on times of about 1 hr accompanied by lower level variations on $\gtrsim 20$ min. These appear as horizontal stripes with significant variations across the 160 MHz. In the secondary spectrum (right panel) power is visible as a function of f_t only at delays $f_\nu = 0$ and 6 nanosec, showing no detectable arc.

The zero delay profile is just the power spectrum of the time variations averaged across the 160 MHz. MdB also plotted such a profile and compared it with the expected power spectrum shape for refractive variations for a screen and extended medium model and found that the observations drop more slowly than expected. The excess at high $f_t \gtrsim 0.015$ cy-
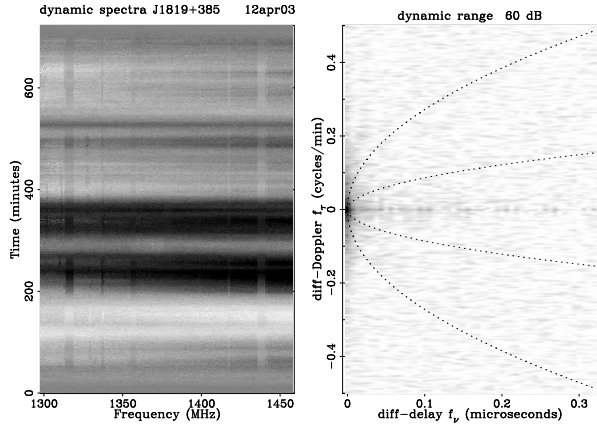
dynamic spectra J1819+385   12apr03

dynamic range 60 dB

Fig. 10. *Left:* Dynamic spectrum of quasar J1819+385 recorded at Westerbork by Macquart & de Bruyn (2005); display format as in Figure 9. On the right the secondary spectrum (S_2) has a logarithmic grayscale over 60 dB. The dotted lines show where an arc would be for screen distances of 5 pc and 50 pc, but no arc is detected.

cles/min was ascribed to diffractive ISS not included in the refractive model. The presence of such rapid ISS is their evidence for a high brightness source component.

I have used a full screen simulation to investigate the effect of source structure on the detectability of arcs at frequencies near the transition from strong to weak scintillation, where the refractive and diffractive approximations may not be valid. I took a transition frequency of 4.4 GHz, which is typical of the MdB models, and for a plane wave source the intensities were computed over a square region for the same frequencies as in the observations. The effect of source structure was modelled by smoothing the intensity patterns over a spatial scale $L\theta_{\mathrm{src}}$, for a range of source sizes. For each of the source sizes the results were saved as dynamic spectra and secondary spectra were computed.

For sources smaller than the critical diameter for DISS arcs are clearly visible, though they are not as sharply defined as in Figure 9. As the source radius is increased the secondary spectra are cut-off for $f_t \gtrsim V/(L\theta_{\mathrm{src}})$. I chose a representative model from those considered by MdB for the observations of quasar J1819+385. It has a compact component of radius $\theta_{\mathrm{src}} = 16\mu$as of mean flux density 150 mJy and scintillates due to a thin layer at distance 15 pc from the Earth. As in the observations the simulation for this model did not show signs of an arc. Instead of displaying the secondary spectra as a grayscale it is more illuminating in such a case to plot cuts

through the secondary spectra at fixed delays. Figure 11 shows cuts at the 3 lowest delays. The upper panel is for the observations (from Figure 10); the center is a simulation for the MdB source model mentioned above; the lower is a simulation for a two-component model as discussed below.

The zero delay cut is the normal 1-dim power spectrum of the variations summed over the total band. MdB showed this for the observations in a log/log format rather than the log/linear format used here. Note that though the observed profile drops steeply from the origin in f_t, it has a broad low level "skirt" out to 0.1 cycles/min at about 3 decades below its peak. Also the profile at 6μsec delay starts more than 2 decades lower but has a similar skirt. It was the power out to 0.1 cycles/min that MdB identified as showing a power law form due to diffractive ISS. In contrast the screen simulation for a single component with all of its flux in a Gaussian source of 16μas (center panel) has a zero delay profile that is wider at the peak and then drops sharply, and the next delay profile is similar but less than one decade lower.

In an attempt to find a screen model that matches the observed profiles I synthesized results for a two-component model consisting of centered Gaussian components with a variable ratio of flux densities. The lowest panel of Figure 11 shows results that are somewhat similar to the observations. The source consists of Gaussian concentric components of radii 16 and 160μas with 10% and 90% of the flux density, respectively. Its peak brightness temperature is 1.3×10^{13}K, about a factor eight less than in the MdB single component model. The simulated profiles agree with the observations in their relative heights at 0 and 6μsec, and each has a broader low level component. However, the zero delay profile does not show the power-law behaviour seen in the observations. The associated dynamic and secondary spectra are shown in Figure 12. The dynamic spectra exhibit slow deep modulations and shallower faster modulations with visible structure across the 160 MHz of the simulation, somewhat like that observed. It is important to note that the simulation includes all of the ISS phenomena (diffractive and refractive) and assumes scattering in a thin layer. The source cut-off for a thin layer provides a steep cut-off in these profiles at fixed delay.

I conclude that it is difficult to match the observations with a screen model, even allowing for a two-component source structure. In attempting to match the observed power-law form of the power spectra, MdB obtained a much closer match with
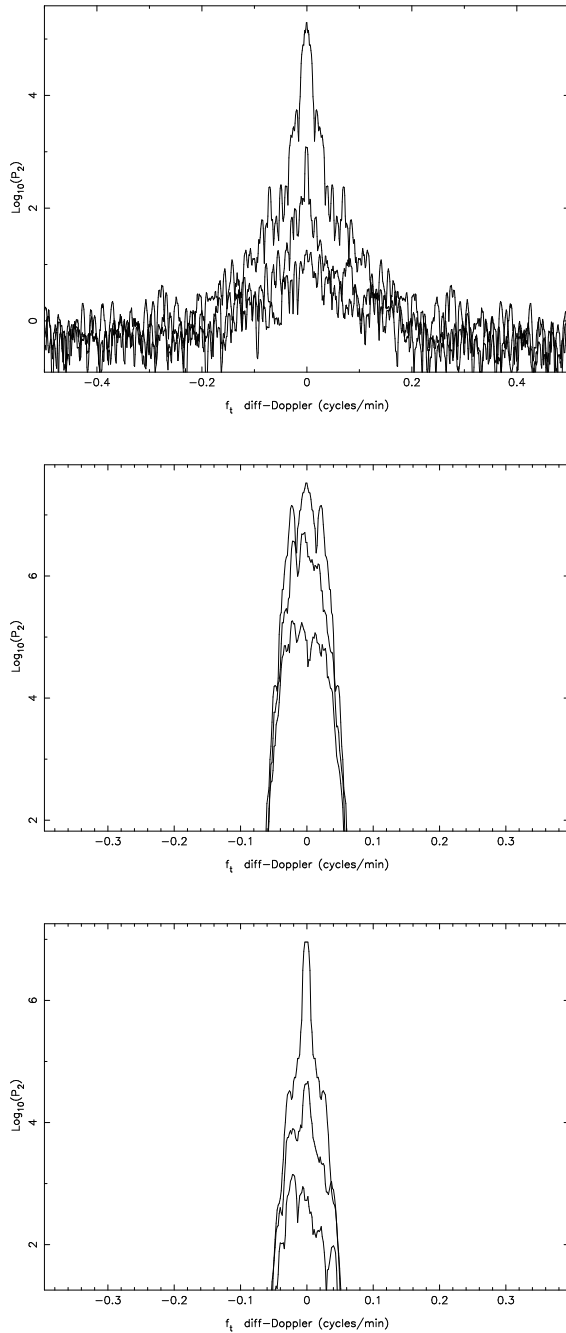
Fig. 12. Simulated dynamic and secondary spectra (displayed as in Figure 9) for a model source with 10% of its mean flux in a source of 16μas radius and the rest in 160μas.

Fig. 11. Cuts through the logarithm of the secondary spectrum at delays of 0, 6 & 12 μsec (in order from highest to lowest lines). Upper: J1819+385 observed on April 12 2003, with the noise floor about 5 decades below the peak; Center: Screen simulation for a single source of radius 16μas; Lower: Simulation for a two-component source radii 16 and 160μas, with 10% and 90% of the flux density, respectively. The plots at zero delay are just the power spectra of the variations when averaged over the 160 MHz bandwidth.
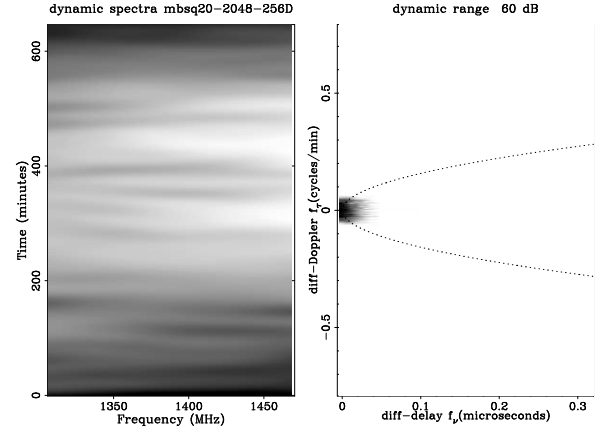
refractive ISS due to scattering in an extended layer that extends to near the Earth. Though the observations still showed an excess over the asymptotic theory, which indicates the influence of diffractive ISS. The basic phenomenon that gives a power law spectrum for refractive ISS in an extended medium is that there is a correlation between the time-scale of the scintillations from each layer and the distance to that layer, so that a range of distances gives rise to a spectrum of timescales. I suggest that the same process is likely to cause a power law widening in the spectrum when the calculation properly accounts for diffractive and refractive phenomena, even though the scintillation power does not add linearly from different distances. Though simulations cannot at present be done for an extended source seen through an extended scattering medium, it should be possible in the near future.

In conclusion, interstellar scintillation is the cause of rapid random variation in the flux density of the compact cores of many quasars and active Galactic nuclei at centimeter wavelengths. There are multiple lines of evidence that support this statement, and the interpretation of ISS allows us to make quantitative estimates for the size of the ultra-compact structure of sources at a resolution finer than can be achieved even with VLBI. The results show that almost all IDV (and IHV) can explained by emission with an intrinsic brightness within the inverse Compton limit – beamed in relativistic jets with Doppler factors in the range 5-75, as is generally concluded from VLBI. There are a very few sources that show IHV which appears to be due to scattering in a region only 5-50 pc from the Earth. The absence of

more IHV sources in the MASIV survey suggests that these near Earth regions cover a relatively small solid angle.

REFERENCES

Armstrong, J. W., Rickett, B. J., & Spangler, S. R. 1995, ApJ, 443, 209

Bignall, H. E., et al. 2003, ApJ, 585, 653

Blandford, R. D., & Narayan, R. 1985, MNRAS, 213, 591

Coles, W. A., Rickett, B. J., Codona, J. L., & Frehlich, R. G. 1987, ApJ, 315, 666

Cordes, J. M., Rickett, B. J., Stinebring, D. R., & Coles, W. A. 2006, ApJ, 637, 346

Cordes, J. M., & Lazio, T. J. W. 2002, astroph-0207156

Dennett-Thorpe, J., & de Bruyn, A. G. 2000, ApJ, 529, L65

—————. 2002, Nature, 415, 57

—————. 2003, A&A, 404, 113

Haffner, L. M., Reynolds, R. J., Tufte, S. L., Madsen, G. J., Jaehnig, K. P., & Percival, J. W. 2003, ApJS, 149, 405

Heeschen, D. S., Krichbaum, T., Schalinski, C. A., & Witzel, A. 1987a, AJ, 94, 1493

Heeschen, D. S., & Rickett, B. J. 198b7, AJ, 93, 589

Jauncey, D. L., & Macquart, J.-P. 2001, A&A, 370, L9

Kedziora-Chudczer, L., Jauncey, D. L., Wieringa, M. H., Walker, M. A., Nicolson, G. D., Reynolds, J. E., & Tzioumis, A. K. 1997, ApJ, 490, L9

Kraus, A., et al. 1999, A&A, 352, L107

Lazio, T. J. W., Waltman, E. B., Ghigo, F. D., Fiedler, R. L., Foster, R. S., & Johnston, K. J. 2001, ApJS, 136, 265

Lovell, J. E. J., Jauncey, D. L., Bignall, H. E., Kedziora-Chudczer, L., Macquart, J.-P., Rickett, B. J., & Tzioumis, A. K. 2003, AJ, 126, 1699

Macquart, J.-P., & de Bruyn, A. G. 2005, A&A, 446, 185 (MdB)

Marscher, A. P. 1998, in ASP Conf. Ser. 144, Radio Emission from Galactic and Extragalactic Compact Sources, ed. J. A. Zensus, G. B. Taylor, & J. M. Wrobel (San Francisco: ASP), 25

Qian, S.-J., Kraus, A., Zhang, X.-Z., Krichbaum, T. P., Witzel, A., & Zensus, J. A. 2002, Chinese J. Astron. Astrophys., 2, 325

Quirrenbach, A., Witzel, A., Krichbaum, T., Hummel, C. A., Alberdi, A., & Schalinski, C. 1989, Nature, 337, 442

Quirrenbach, A., Witzel, A., Kirchbaum, T. P., et al. 1992, A&A, 258, 279

Rickett, B. J. 1986, ApJ, 307, 564

Rickett, B. J., Coles, W. A., & Bourgois, G. 1984, A&A, 134, 340

Rickett, B. J., Quirrenbach, A., Wegner, R., Krichbaum, T. P., & Witzel, A. 1995, A&A, 293, 479

Rickett, B. J., Kedziora-Chudczer, L., & Jauncey, D. L. 2002, ApJ, 581, 103

Rickett, B. J., Lazio, T. J. W, & Ghigo, F. D. 2005, ApJ, 165, 439

Rickett, B. J., Witzel, A., Kraus, A., Krichbaum, T. P., & Qian, S.-J. 2001, ApJ, 550, L11

Stinebring, D. R., McLaughlin, M. A., Cordes, J. M., Becker, K. M., Espinoza Goodman, J. E., Kramer, M. A., Sheckard, J. L., & Smith, C. T. 2001, ApJ, 549, L97

Taylor, J. H., & Cordes, J. M. 1993, ApJ, 411, 674

Wagner, S. J., et al. 1996, AJ, 111, 2187

Waltman, E. B., Fiedler, R. L., Johnston, K. J., Spencer, J. H., Florkowski, D. R., Josties, F. J., McCarthy, D. D., & Matsakis, D. N. 1991, ApJS, 77, 379

Barney J. Rickett: Department of Electrical & Computer Engineering, University of California, San Diego, CA 92093-0407, USA (bjrickett@ucsd.edu).